Proceedings of the ENC-GNSS 2014, the
European Navigation Conference, Rotterdam,
The Netherlands, April 15-17, 2014

DriftLess™, an innovative method to estimate and compensate for the biases of inertial sensors.

Marcel Ruizenaar, Rob Kemp
TNO Technical Sciences, The Hague, The Netherlands,
marcel.ruizenaar@tno.nl, rob.kemp@tno.nl

Abstract: In this paper a method is presented that allows for bias compensation of low-cost MEMS inertial sensors. It is based on the use of two sets of inertial sensors and a rotation mechanism that physically rotates the sensors in an alternating fashion. After signal processing, the biases of both sets of sensors are estimated and compensated for, resulting in a virtually bias free inertial sensor. A demonstrator has been build. First results with a test of the demonstrator in an airborne application show that the bias of low-cost MEMS gyroscopes can be reduced to less than 20 deg/hr. Further improvements up to a 2 deg/hr level are demonstrated in the laboratory. Lab-tests have shown that the bias of low-cost accelerometers can be reduced to below 0.1 mg.

BIOGRAPHY

Marcel Ruizenaar is working for twenty seven years at TNO, an independent research organization for applied scientific research, located in the Netherlands. The first two decades he has been involved in research on guidance and navigation systems of guided weapons. The last five years he is responsible for setting up a research group on Robust Navigation with focus on indoor navigation. He is inventor of several patented localization concepts, sensor improvements and new sensor concepts. Rob Kemp is working for thirty three years at TNO. He has been involved in research on and valorization of electro optical processing algorithms and automatic video analysis. He is now responsible for the valorization of the Robust Navigation techniques.

1 INTRODUCTION

It is well known that inertial navigation systems (INS) drift over time. Primarily, this drift is caused by unknown and in time fluctuating offsets (the so-called biases) on the outputs of the inertial sensors (also known as the inertial measurement units or IMU's). After initial bias calibration, the remaining biases (a sum of fixed and time varying biases) cannot be calibrated out and can only be estimated and compensated for with aiding information from other sensors. Especially if low-cost Micro-Electro-Mechanical-Systems (MEMS) based inertial sensors are used, the drift of an INS due to the unknown biases is extremely high, making the un-aided use of an INS system impractical [El-Sheimy 2008].

A combined system that uses INS as a primary system and a Global Satellite Navigation System (GNSS) as an aiding system is the INS/GNSS integrated navigation system. Well known combinations of INS with GNSS are the so-called "Loosely coupled", "Tightly coupled" and "Deeply coupled" integrated navigation systems, the names referring to the way the coupling of the INS with the GNSS system is done. Using these integrated systems, the inertial sensor biases are only very indirectly observable [Groves 2008, pp.398]. As a result, such a combined system can only compensate for the inertial sensor biases with a limited accuracy, given the relatively fast and unknown changes of the bias. When aided by GNSS, these low-cost INS/GNSS systems can overcome only but the shortest GNSS outages. Errors in the order of 50 m after 20 seconds of un-aided use are common [George 2005]. The use of better IMU's, especially better gyros, with lower biases, directly results in longer un-aided use of the INS and makes the INS/GNSS system more robust.

A method is presented in this paper that compensates for the biases of inertial sensors without any aiding of additional sensors like GNSS. It is based on rotating the input signal but leaving the bias unchanged. Physically this is done by making use of two sets of inertial sensors and a rotation mechanism that physically rotates the sensors with respect to a common body axis system in a

known alternating rotation scheme. After some signal processing, the biases of both sets of sensors are estimated and subtracted from the sensors, resulting in a virtually bias free inertial sensor. Among the interesting properties of the method are the continuous estimation of the biases of inertial sensors during operational use and the resulting independence of temperature.

In the paper, the basic principles are addressed and, a practical set-up is presented along with test results in an airborne application.

2 DRIFTLESS™

In this section, the bias estimation method will be presented. It is given the name DriftLess, referring to the reduction of the drift in INS systems. The method is patented [Ruizenaar 2012].

2.1 Basic principle of DriftLess™

The DriftLess method uses two sensors. Each sensor measures the physical quantity $\bar{x}$. See Figure 1 for a block diagram of the basic principle of the method. This quantity may be acceleration or rotation rate, but the method can also be used with other types of sensors like magnetometers, in which case $\bar{x}$ is a magnetic field. So the method is not limited to inertial sensors. $\bar{x}$ is a vector relative to a common body axis system. In the following step-wise approach, the basic principle is explained.

As a first step, each sensor is mechanically rotated by a proper rotational means (e.g. a motor, actuator etc.). Rotating the sensor is equivalent with multiplying $\bar{x}$ with a rotation matrix R_i, with i=1 or i=2 for sensor 1 or 2. These rotation matrices represent the relative rotation of the sensor with respect to the common body axis system. Rotation of a sensor is done in a single plane of rotation, controlled by some controller (not shown in Figure 1) and are known at all times. Its effect can therefore be undone by means of signal processing by multiplying the sensor signals with the inverse matrices R_i^{-1}.

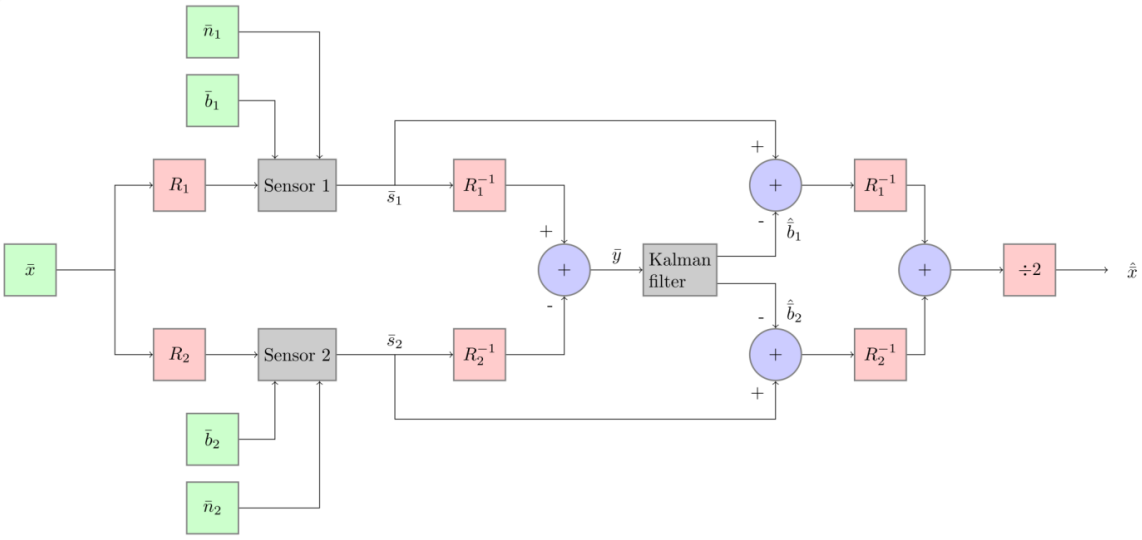

Figure 1. Basic principle of DriftLess. Two sensors are rotated in an alternating fashion. Each sensor measures a physical quantity $\bar{x}$. The rotation of a sensor is equivalent with multiplying with a rotation matrix R_i. After numerically reversing the rotation by multiplying with the inverse matrix, both sensor signals are subtracted. This generates a measurement signal from which a Kalman Filter can estimate the biases of the sensors.

In the second step, the signals are subtracted from each other. As can be seen from the signal flow in Figure 1, the difference signal is independent of the input signal, as both signals paths cancel each other. The difference signal therefore depends only on the biases. The noise of both sensors are independent white noise sources. Multiplying them with the inverse rotation matrices does not further color them [vanderHall 2013].

The difference signal can therefore be expressed as:

$$\bar{y} = R_1^{-1}\bar{b}_1 + R_2^{-1}\bar{b}_2 + \bar{n}$$

In which $\bar{b}_1$ and $\bar{b}_2$ are the sensor biases to be estimated and $\bar{n}$ is the combined noise of both sensors. The planes in which the sensors rotate are preferably orthogonal to each other, but this is not required. The sensors are each rotated in an alternating fashion back and forth between two angular positions. These positions are preferably +/- 90 degrees for each sensor. So sensor 1 is rotated from -90 degrees to +90 degrees. After some time, sensor 2 is rotated from -90 to +90. Then sensor 1 is rotated back from +90 to the -90 position, and finally, sensor 2 is rotated back from +90 to -90. This process is repeated continuously. This process generates four individual states (S1=-90, S2=-90; S1=+90, S2=-90; S1=+90,S2=+90; S1=-90, S2=+90). Each individual state is represented by a unique combination of rotation matrices.

The third step of the signal processing consists of a Kalman Filter (KF) to estimate the biases from the difference signal. As there are four individual states, all biases are observable [Ruizenaar 2013, vanderHall 2013]. The outputs of the sensors are compensated for the biases and combined. The resulting signal is largely undone from biases and presents the input quantity $\bar{x}$ with high reliability. Further details about for instance the KF can be found in [Ruizenaar 2013].

Figure 2 below further show the schematic overview of the DriftLess technology.

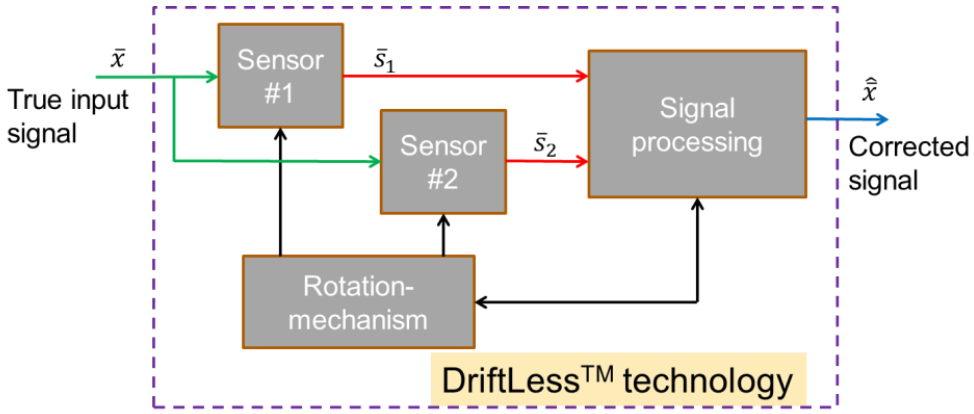

Figure 2. Schematic overview of the DriftLess technology. Two sensors are rotated by a rotation mechanism. Sensor signals and information about the angular position of the sensors are used in a signal processing block to estimate the biases and correct the sensors for it.

2.2 Demonstrator of DriftLess™

The first laboratory demonstrator of DriftLess is described in [Ruizenaar 2013]. This demonstrated the bias compensation method and already gave good results. However, for several reasons it was not robust enough to be used in practical tests. Therefore a new demonstrator was build, of which a photo is presented in Figure 3. This demonstrator version uses very low-cost inertial sensors from Invensense (MPU6050), two Voltz DA22-12-2615 servo motors, a couple of miniature ball bearings and a signal processing board. The demonstrator further contains a low-cost Global Positioning System (GPS)-receiver (uBlox LEA 6), micro SD-card data storage and a BPM085 barometer. This version of the demonstrator only records all sensor data and stores it on the internal SD-card or transmit it real-time to a computer via a build–in serial (RS232) to USB converter.

Only external power need to be applied, optionally a GPS-antenna and optionally a USB-cable to operate the demonstrator. The USB-cable is only required if data is not stored on the SD-card. Average power consumption is approximately 1 W. This power consumption is expected to be further reduced in future versions. Approximate size of the demonstrator is 1.5 dm^3. A further size reduction to approx. 25 cm^3 is expected in the near future.

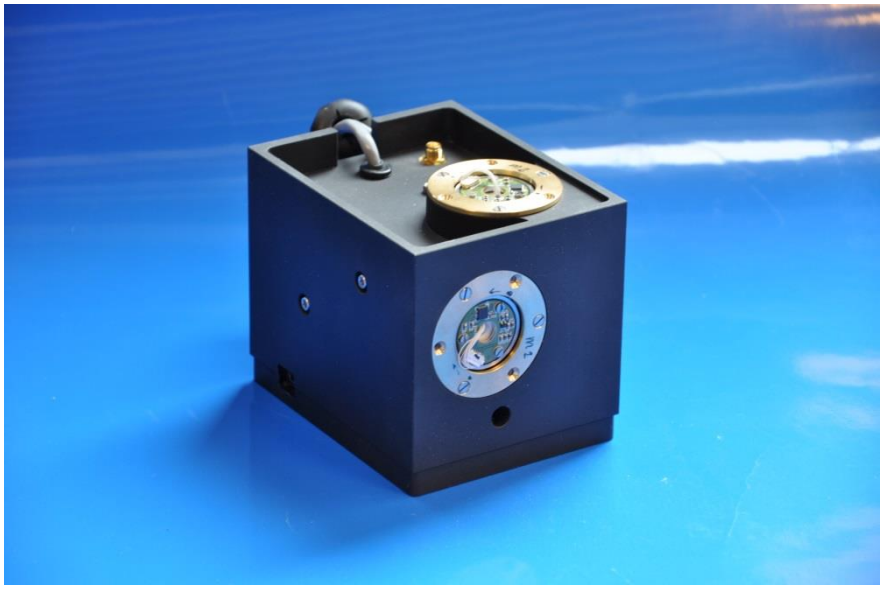

Figure 3. Photo of the DriftLess demonstrator. The photo clearly shows two sensor PCB's that can be rotated in two planes, orthogonal to each other.

As an example, Figure 4 below in the left plot shows the low-pass filtered output of the 6 individual gyroscopes of the DriftLess demonstrator. A low-pass filter is used to reduce the wide band noise which would otherwise make the plot very unclear. The data is taken during a stationary period and at constant temperature. The sensors were not rotating, so the DriftLess technology was not used to estimate the biases. The plot is already corrected for the enormous turn-on bias, which is in the order of a few thousand deg/hr. The plot therefore only shows the in-run bias fluctuations. Earth rotation rate which is also measured by the gyros is also removed from the plot.

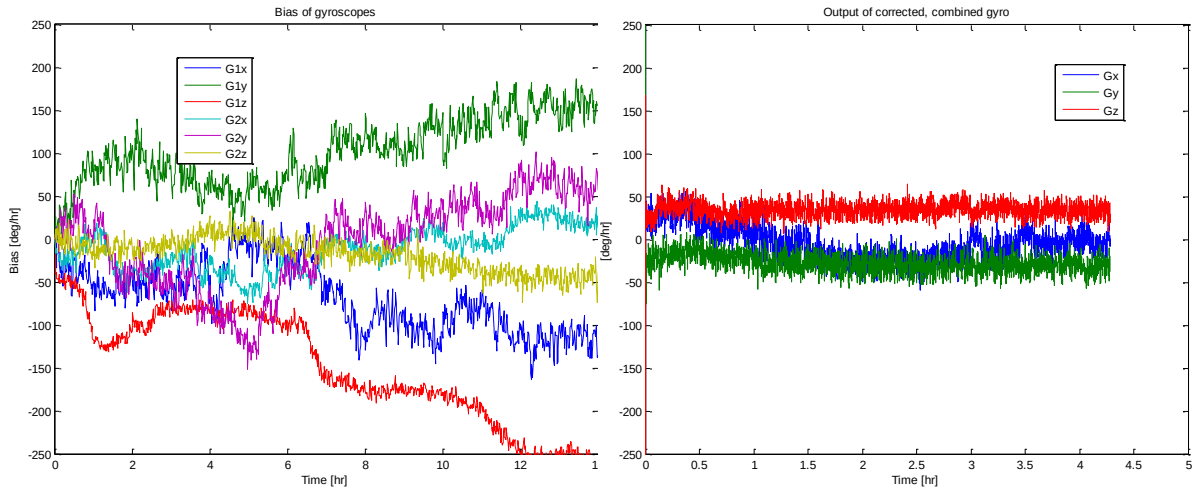

Figure 4. Plot on the left: example of low-pass filtered output of the 6 individual gyroscopes of the DriftLess demonstrator. The data was taken during a stationary period and at constant temperature. The sensors were not rotating. The plot is already corrected for the enormous (un-calibrated) turn-on bias. Plot on the right: example of low-pass filtered output of the combined gyros, corrected for biases by DriftLess. The enormous turn-on biases were automatically estimated and corrected for.

The plot on the right in Figure 4 shows an example of the corrected output of the combined gyro of the DriftLess demonstrator. In this case, the DriftLess method was used to correct the biases. To further reduce the noise, low-pass filtering is applied. In this situation, the demonstrator was also stationary and at constant temperature. DriftLess was however operating and the sensors were rotating. The enormous turn-on biases were automatically estimated and compensated for by

DriftLess. The plot clearly shows that most of the in-run bias fluctuations are also compensated. Part of the non-zero output is due to the measured Earth rotation which is obviously not removed by DriftLess. Most of the non-zero output is probably caused by un-calibrated g-dependent offsets of the gyros. These apparent limitations to the bias estimation are currently investigated. Further improvement of the demonstrator should make the residual bias much smaller, in the order of 2 deg/hr. First lab-tests indicate that this should be possible.

It is known that the biases of inertial sensors are very dependent on temperature. Partially, temperature dependent biases can be calibrated out. Still, large temperature effects remain. As long as these bias changes are slow time varying changes, they are automatically compensated for by DriftLess. To some extend this also applies to vibration depending bias changes and bias changes due to shock. At least theoretically, all these effects should be much less. This matter is still subject of research.

2.3 Allan Variance of the demonstrator

The time varying bias and noise are probably the most dominant inertial sensor error sources. A lot of methods have been devised to characterize these error sources. The simplest is the Allan variance (AV). The AV is a method of representing the root means square (RMS) random drift error as a function of averaging time. It is simple to compute and relatively simple to interpret and understand [El-Sheimy 2008]. This time domain characteristic of the noise of a sensor was first introduced to analyze the precision of oscillators for time measurements [Allan 1966], but has been widely applied to characterize the accuracy of inertial sensors [El-Sheimy 2010, Yuksel 2010].

In Figure 5 below, on the left, a plot is made of the AV of the six individual gyroscopes in the DriftLess demonstrator. The left part of the plot is mainly characterized by a line going straight down. This line stands for the white uncorrelated part of the noisy sensor output. The part of the plot on the right is due to the time varying bias, the correlated part of the noisy sensor output. A complete understanding of different aspects of the AV are beyond the topic of this paper. As far as the DriftLess technology is concerned, it suffices to say that under ideal circumstances, the DriftLess technology estimates and compensates all time varying biases, leaving only white uncorrelated noise at the output of the sensor. Effectively this means that the AV of the ideally compensated sensor is characterized by only a straight line as indicated in Figure 5 by the dashed black line. In this ideal situation, the AV has no minimum.

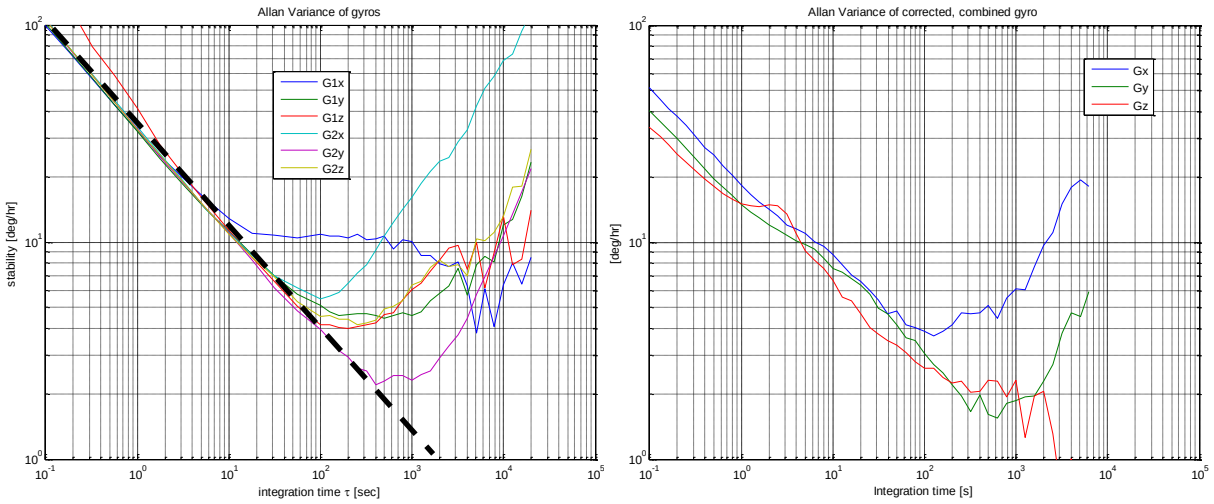

Figure 5. Plot on the left: the Allan Variance (AV) of uncorrected low-cost MEMS gyros. The dashed black line is the best situation achievable, it represents a sensor with only pure white noise. At higher integration times, the curve goes up. That part represents the bias fluctuations. Plot on the right: the AV of the corrected gyro output of the DriftLess demonstrator. As can be seen, most of the in-run bias fluctuations are reduced, but the result is still not optimal.

In Figure 5, on the right, the AV is plotted of the combined corrected gyro signal as output by the DriftLess demonstrator. The axes of both plots are the same. Both plots correspond with the time plots in the previous Figure 4. As can be seen from Figure 5, the curves have dropped a bit. This is mainly due to the fact that the noise of both sensors are combined which gives a reduction of a factor $\sqrt{2}$. For the same reason, the minimum of the curve (which ideally should not exist anymore) is reduced with the same factor. As can be seen in the right plot of Figure 5, the Gx-signal still has much bias variation. Also the Gy-signal has some residual variation. These are probably due to a number of effects.

1. Uncalibrated g-dependent effects, which are clearly visible in the raw sensor data. It is known that MEMS gyros are sensitive to g-forces, vibrations etc. These effects have not been calibrated and are a function of temperature. It can be shown that (some) g-dependent effects cannot be separated from biases by the KF. It should be possible to largely calibrate out these effects. Any remaining g-sensitive effects will pose a limit to the capabilities of DriftLess.
2. Mechanical vibrations of the rotation of one sensor, sensed by the other. These effects are also clearly visible in the raw sensor data and will largely be eliminated in future designs.
3. Temperature dependent stress-effects.

Further detailed discussion of these effects, which are still under investigation, is beyond the scope of this paper.

Although the AV is still not optimal, much reduction of in-run bias variation can be observed. Besides this reduction, the total turn-on bias is eliminated, leaving the turn-on bias an obsolete parameter specification.

2.4 Properties of DriftLess™

Summarizing this section, some of the interesting properties of the DriftLess technology are:

- It can estimate and compensate for the biases of sensors that measure a vector quantity. This can be inertial sensors like accelerometers and gyroscopes, but also magnetometers, gravimeters, windmeters etc. Whenever such a sensor exhibits an unknown bias, it can be estimated by DriftLess.
- Bias estimation can be done continuously during operational use.
- Turn-on biases (also called the DC or static bias) are completely eliminated.
- Most of the in-run biases are eliminated.
- Theoretically, only white noise remains.
- It is known that the bias heavily depends on temperature. As long as temperature changes are slow in time, this dependency vanishes using DriftLess as the bias is almost completely eliminated.
- Sudden bias changes of the uncorrected sensor due to for instance shock (a well-known phenomenon with accelerometers) are automatically compensated for by DriftLess.
- Bias changes due to vibration [Yuksel 2010] are automatically compensated for.

2.5 Calibration

Before the DriftLess demonstrator can be used, it needs to be calibrated. Calibration of inertial sensors generally consists of finding the coefficient for the bias, scale factor and misalignment [Artesea 2008]. In our case, it is obvious that the bias calibration can be omitted as this is the main purpose of DriftLess to do this job during operational use. The remaining scale factor and misalignment calibration can all be combined by finding all the elements of a single matrix, corresponding to the matrix R_i of Figure 1. Further details about this correspondence can be found in [Ruizenaar 2013].

The elements of the 3x3 matrix can be found by utilizing a 6-position procedure in which the demonstrator is brought in six different known angular positions. In our case the demonstrator was alternately switched from -90 to +90 degrees using the very accurate stepper motor of a Computer Numerical Control (CNC) machine (see Figure 6 on the left), used in our precision mechanic workshop. The demonstrator was mounted such that the axis of rotation by the CNC machine was perpendicular to the XY-surface of the demonstrator box. Then the demonstrator was mounted to the CNC machine with another surface and the procedure was repeated. This was done for all three possible surfaces (XY, XZ, YZ), resulting in six different angular positions.

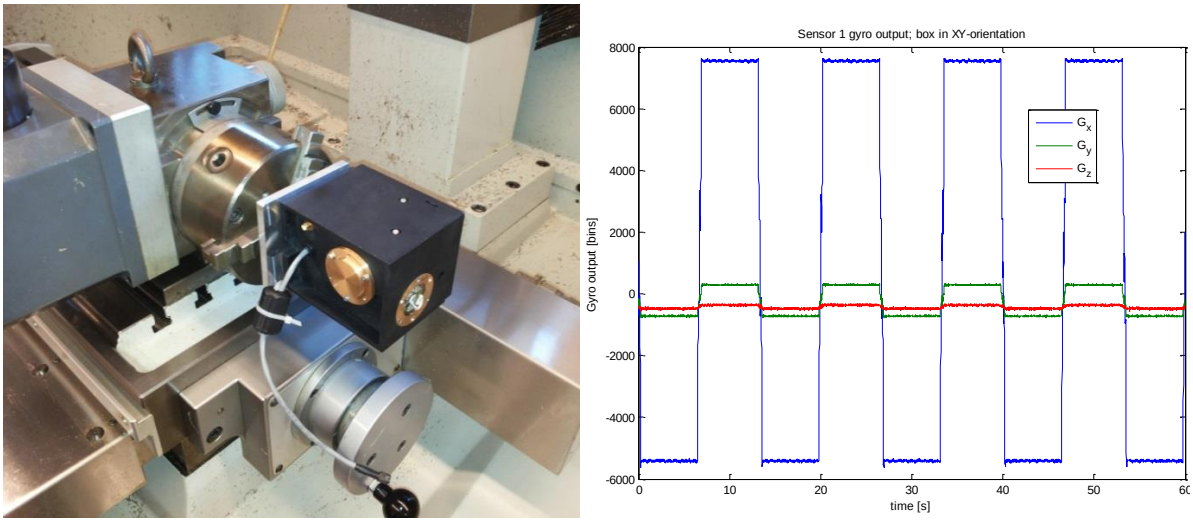

Figure 6. Plot on the left: A CNC machine used to calibrate our DriftLess demonstrator.The machine alternately rotates the whole box from -90 to +90 degrees with constant known speed. This alternating reference signal is used to find the coefficients of the rotation matrices R_i. Plot on the right: an example of the recordings of the gyroscopes during the calibration.

During the alternate switching from -90 to +90 degrees, the rotation rate was constant and accurately known. In the case of the accelerometers, the demonstrator remained stationary for a short period in each angular position. Because of the alternate switching, the output of the gyroscopes and accelerometers varies. The plot in Figure 6 on the right shows an example of the output of the gyros with the demonstrator in the XY orientation. The difference between the top/bottom values are a direct measure of the coefficients of the matrix R_i. For further details see [Ruizenaar 2013].

3 INS/GNSS INTEGRATED NAVIGATION SYSTEM

Combining an INS with a GNSS is a well-known method to overall increase the accuracy and bandwidth of the GNSS and at the same time reduce the drift of the INS. By combining of INS and GNSS some disadvantages of the individual systems vanish and the combined system benefits from the advantages of each individual system. The general layout of an integrated navigation system that uses information from other sensors to bound the drift of an INS is given in Figure 7. An INS, fed by IMU data, acts as the main navigation system. The measurements of supporting sensors (e.g., position output or Pseudo Range (PR) output by a GNSS receiver, height measurements of a barometer of Doppler data of a Doppler Velocity Log) are predicted based on the INS output (position, velocity and attitude). The difference between predicted measurements and actual measurements are input to a navigation filter Usually a KF is used as the navigation filter. The KF estimates the errors of the INS position, velocity and attitude (9 states). Also it estimates the 6 states consisting of the IMU errors (the accelerometer and gyro biases). This totals to 15 error states. Besides these 15 states, the KF usually also estimates the GNSS receiver clock bias and drift, resulting in 2 additional states.

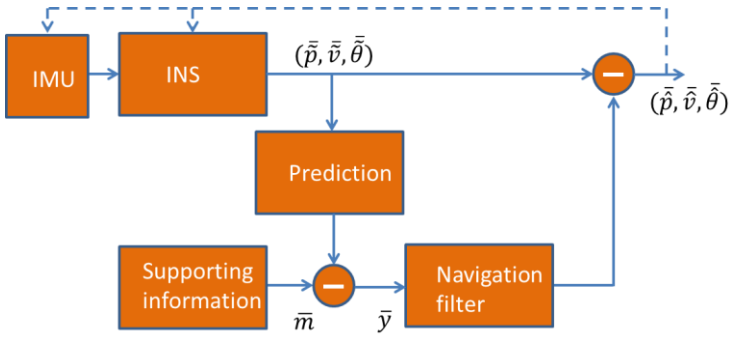

Figure 7. General lay-out of an integrated navigation system that uses information from other sensors to bound the drift of an INS.

Details about the principles of such a combined INS/GNSS navigation system are beyond the scope of this paper. The interested reader is referred to [Groves 2008], in which many other filter configurations are presented having even more states to be estimated.

Position and velocity measurements of the GNSS receiver are directly related to the position and velocity errors of the INS. The KF can therefore estimate these errors very quickly. In the same way, Doppler and PR measurements of the GNSS receiver are also directly related to the INS position and velocity errors. INS attitude error and the IMU biases are however not directly observable from the GNSS measurements. Estimating these errors is done in a very indirect way by the KF [Groves 2008, pp.398]. The quality of estimation therefore depends on sensor noise, GNSS measurement noise, system model noise, number of states to be estimated etc. These noise sources effectively set the bandwidth of the KF. In simulations, the bias is often taken as a random value, fixed in time. Eventually, such a fixed bias will be estimated if the simulation lasts long enough. The biases are however not constant but vary in time.
The quality of IMU bias estimation is therefore limited in an INS/GNSS integrated navigation system. In general only a large part of the turn-on biases are estimated. In [George 2005] practical test results are reported of a combined INS/GNSS navigation system, based on low-cost MEMS IMU's, in a UAV application. The results show that the gyro bias is estimated up to an approximate 100 to 200 deg/hr. These figures are not directly mentioned in the paper, but are calculated back from the reported drift using the formula:

$$P_{drift} = \frac{1}{6} b_g g_0 t^3 \qquad [1]$$

in which P_{drift} is the reported drift during a simulated GNSS-outage, b_g is the gyro bias, g_0 is the gravity (9.8 m/s^2) and t is the time duration of the simulated outage.

Un-estimated sensor biases reduce the overall quality of the navigation solution, and more important, the navigation system will drift during GNSS-outages. The DriftLess technology estimates the biases of the inertial sensors independent of the GNSS measurements. Combined with an INS/GNSS integrated navigation system, this gives some additional interesting properties.

- All inertial sensor biases are estimated by DriftLess. The INS/GNSS system does not need to estimate them and the number of error states of the KF can be reduced from 15 to 9 (excluding the clock states). This improves the quality of the remaining states and reduces the required numerical processing capabilities.
- Bias estimation will be much better than when estimated by the INS/GNSS system. Theoretically, all bias will be removed.
- Although DriftLess contains its own KF, the output of the corrected sensors only contains white noise (theoretically). Therefore no performance will be lost due to possible correlated noise entering the INS/GNSS system. From this point of view, the combined DriftLess/INS/GNSS navigation system seems to work optimal.

4 FIELD TESTS SET-UP

In May 2013, a field test was done. The main goal of this test was to investigate the imaging behavior of a Synthetic Aperture Radar (SAR). Details about this test, the SAR imaging system and results are described in [vanderGraaf 2013]. As in most mobile radar applications, compensating for the dynamics of the vehicle, in this case a small airplane, is mandatory. Using an INS and IMU's is the only option in practice. A combined INS/GNSS integrated navigation system based on high quality IMU's could have been used to do this task. The test is however part of the development of a small SAR system for Unmanned Aerial Vehicles (UAV's) in which only preferably low-cost miniature inertial sensors are to be used, in combination with low-cost GNSS receivers. The use of our DriftLess system, which is expected to be further miniaturized in the near future and makes use of low-cost components, is then a logical step.

Figure 8. Small airplane used for the SAR imaging tests. A pod was mounted below the left wing. DriftLess was placed in the front of the pod

The SAR system and the DriftLess system were both build in a pod. Figure 8 shows the pod, mounted under the wing of a small airplane. The black surface is the antenna of the SAR radar, slightly directed downward. The DriftLess system was placed in the front of the pod. During the flight all signals of the IMU's of Driftless were recorded, together with the GPS Pseudo Range and Doppler signals and SAR radar data. Afterwards, in the laboratory, the signals were processed and combined.

We didn't equip the airplane with expensive devices to measure absolute ground truth. We therefore took the blended INS/GNSS solution with full satellite visibility to be the baseline "ground truth" solution. After finding the baseline solution, the calculations were repeated and during some parts of the trajectory, GNSS signals were omitted from the calculations. During these intervals, the INS started to drift in position, velocity and attitude. This drift was observable by subtracting the baseline solution. Based on the observed drift in position, an equivalent gyro bias can be calculated from formula (1) mentioned before. Off course, it is possible that the drift is not the result of only gyro biases. Also accelerometer biases, angular random walk (ARW), velocity random walk (VRW), attitude errors and velocity errors may contribute to the drift. ARW and VRW contribute only minor errors and can safely be ignored. Equivalent accelerometer biases can be calculated using:

$$P_{drift} = \frac{1}{2} b_a t^2 \quad [2]$$

In which b_a is the equivalent accelerometer bias.

5 RESULTS

This section reports the results of combining DriftLess with an INS/GNSS integrated navigation system. Results are reported in terms of equivalent residual gyro bias. That is, the residual gyro bias is not measured directly but can be calculated based on observed drift. Results of SAR data processing and the benefits of using DriftLess to SAR data processing are not discussed here. The interested reader is referred to [vanderGraaf 2013].

During the test flights, the IMU data of DriftLess was recorded along with GNSS Pseudo Range data, GNSS Doppler data and barometer data. These were blended using a so-called Tightly Coupled integrated navigation filter approach having only nine states and two additional states for the GNSS receiver clock and clock bias. Using this type of navigation filter, the output of the stand-alone navigation filter of the GNSS receiver is bypassed. Only the raw data of the GNSS receiver, the Pseudo Range and Doppler signals, are used. The calculated position and/or velocity output of the receiver is ignored. This type of filter has improved performance [Groves 2008] over for instance the so-called Loosely Coupled filter, that only uses the position and/or velocity output of the GNSS receiver.

The output of the GNSS system is drift free over long periods of time but lacks short time accuracy. An INS drifts over longer periods but is accurate for short time periods. The blended INS/GNSS solution combines the best of both worlds, is accurate for short periods and drift free. Figure 9 shows the filtering capabilities of the INS/GNSS integrated navigation system. The green line is the blended INS/GNSS solution, drift free over long periods of time and accurate at short time periods. The blue

line is the position calculated by triangulating the corrected PR measurements, and is equivalent to the position calculation of the GNSS receiver. It clearly shows this solution is drift free in the long term, but misses short term accuracy. The position solution shows large errors at some points and is rather noisy. The integrated solution on the other hand is noise free and drift free.

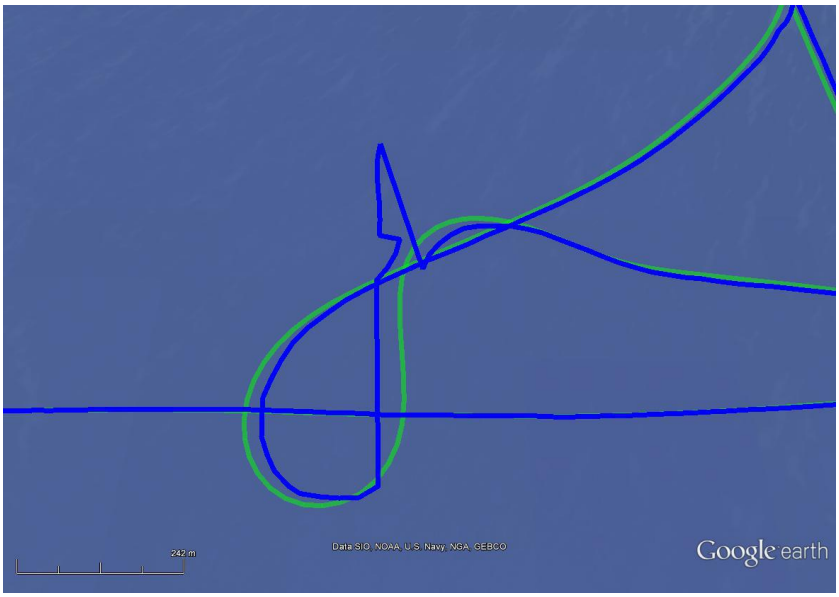

Figure 9. Plot showing the filtering capabilities of the INS/GNSS integrated system. The blue line shows the position based on triangulating the corrected Pseudo Range signals. In the air, GNSS systems are not heavily disturbed (due to for instance Multi-path) as is usually the case on ground. It does however occur. In this part of the trajectory, the triangulation shows a non-smooth flight path. The green line is the filtered smooth INS/GNSS trajectory. The disturbances have completely vanished, showing the benefits of the combined system.

As mentioned before, the blended INS/GNSS solution with full satellite visibility was taken as the baseline “ground truth” solution. We selected a portion of the recorded signals during which the plane was stationary. Figure 10 shows an example of such a situation.

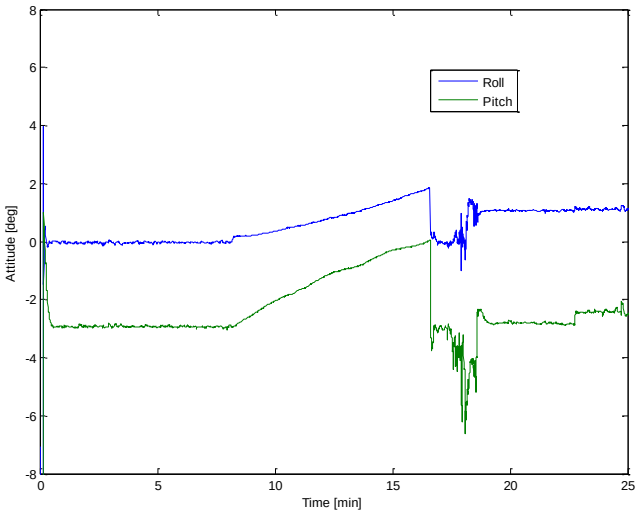

Figure 10. The airplane was stationary and the roll and pitch angles were estimated by the integrated navigation system. During some period of almost eight minutes, the GNSS signals were omitted from the dataset letting the INS drift. This drift can only be caused by uncompensated gyro biases. As can be seen the gyro bias varies during the time interval, but is on the average approximately 20 deg/hr.

In the plot, the attitude (roll, pitch) of the INS/GNSS system is given. After a short time, the output was fully stabilized and remained constant. DriftLess was fully operational and was correcting the accelerometer and gyro biases. GNSS signals were used to find the position, velocity and attitude errors. Each second, the INS was reset with the new solution. After approximately eight minutes, we omitted the GNSS signals from the calculations. Due to remaining, uncorrected gyro biases, the attitude starts to drift. This can be seen in the plot. From it, we can estimate the gyro bas to be in the order of 20 deg/hr. This observed drift can only be attributed to the gyro biases. As no information is entering the KF it is coasting and effectively being bypassed. After approximately seventeen minutes, the GNSS signals were input again to the filter and the output quickly stabilizes back to the original values.

As another example of estimating the residual gyro biases, see Figure 11. In the plot on the left the actual trajectory of the plane is plotted using Google Earth. This trajectory is the output of the INS/GNSS system. Part of the trajectory, indicated by the red circle, is zoomed in and shown at the right side of the figure. Again, the green line is the baseline trajectory with full satellite visibility. During part of this trajectory, for approximately 90 seconds and 3 km of flight, GPS measurements were omitted from the INS/GNSS filter and the INS starts to drift. This INS-only position is indicated by the red line in the right plot of Figure 11. The drift can be measured (approximately 100 m) by comparing with the baseline and, using formula 1, the equivalent gyro bias can be calculated from it, following the same procedure as in [George 2005]. Again the gyro bias is in the order of 20 deg/hr. As an alternative, an equivalent accelerometer bias can be calculated using formula 2. The equivalent accelerometer bias would then be in the order of 3 mg. As we have already demonstrated that DriftLess is capable of estimating the accelerometers biases up to 0.1 mg, the accelerometer bias is not likely to be a major source of the drift. For the same reason, we can derive that equivalent roll or pitch attitude errors are to be in the range of 3 mrad which is also very unlikely.

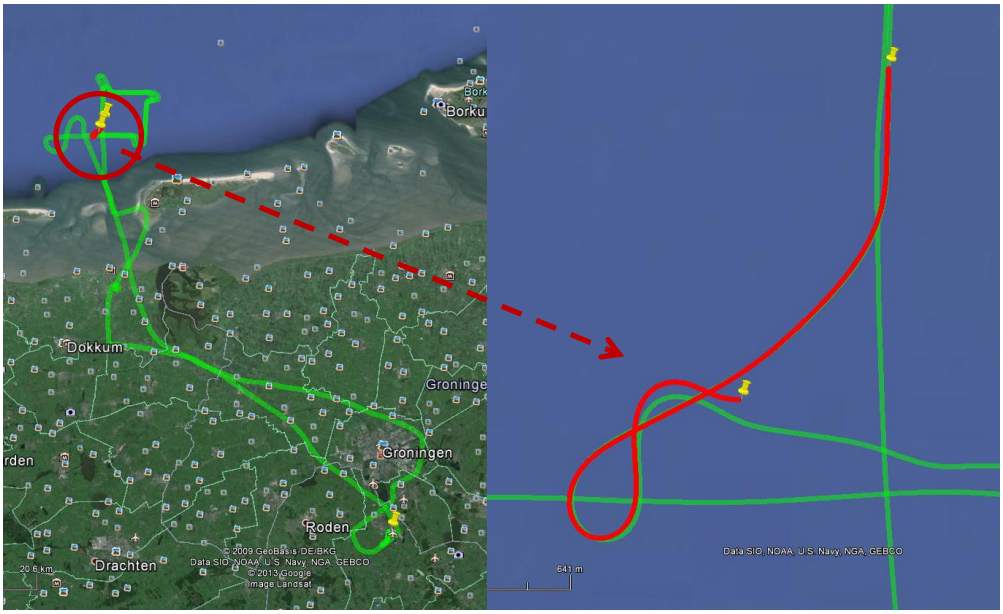

Figure 11. Plot on the left: screen dump of Google Earth, showing the baseline INS/GNSS trajectory of the airplane. Plot on the right: a zoomed-in portion of the trajectory. During approximately 90 seconds, corresponding to a 3 km flight path, GPS signals were omitted from the INS/GNSS filter. The INS then starts to drift (red line).

6 CONCLUSIONS

- Our DriftLess technology can continuously estimate and compensate for the biases of sensors that measure a vector quantity. This can be inertial sensors, but also magnetometers, etc.
- DriftLess properly estimates bias changes due to temperature. As such, DriftLess corrected sensors are no longer temperature dependent.
- The technology is validated in an airborne application.
- The results show that the bias of very low cost MEMS gyroscopes can be reduced to below 20 deg/hr. It's expected that it will be possible to further reduce it to a 2 deg/hr level, which is comparable to some low-end laser gyros. The same method is used to estimate and compensate the biases of low-cost accelerometers up to a 0.1 mg level.

REFERENCES

[1] D.W. Allan (1966). Statistics of atomic frequency standards. Proceedings of the IEEE, vol.54, no.2, pp.221–230

[2] G. Artesea, A. Trecroci (2008). Calibration of a Low Cost MEMS INS Sensor For an Integrated Navigation System, in proceedings of The International Archives of the Photogrammetry, Remote Sensing and Spatial Information Sciences, Vol. XXXVII, Part B5, Beijing 2008.

[3] Naser El-Sheimy, Haiying Hou, and Xiaoji Niu (2008). Analysis and Modeling of Inertial Sensors Using Allan Variance, IEEE transactions on instrumentation and measurement, vol.57, no.1, pp140-149.

[4] Naser El-Sheimy Y. Yuksel and A.Noureldin [2010]. Error modeling and characterization of environmental effects for low cost inertial MEMS units, in proceedings of the IEEE/ION PLANS, Palm Springs, California, 2010.

[5] M. George, S. Sukkarieh (2005). Tightly Coupled INS/GPS with Bias Estimation for UAV Applications, in proceedings of the Australasian Conference on Robotics and Automation (ACRA), Sydney, Australia, December 5-7, 2005.

[6] M.W. van der Graaf, M.P.G. Otten, A.G. Huizing, R.G.Tan, M. Caro Cuenca, M.G.A Ruizenaar (2013). AMBER: An X-band FMCW Digital Beam Forming Synthetic Aperture Radar for a Tactical UAV, in IEEE International symposium on Phased Array Systems & Technology, Boston USA, pp.165-170.

[7] P.D. Groves (2008). Principles of GNSS, inertial, and multi-sensor integrated navigation systems, ISBN-13: 978-1-58053-255-6

[8] Elwin van der Hall [2013]. Error detection and reduction within DriftLess™. M.S. thesis, TNO, The Hague, The Netherlands.

[9] M.G.A. Ruizenaar, Elwin van der Hall, and Martin Weiss (2013). Gyro bias estimation using a dual instrument configuration, in proceedings of the EuroGNC 2013, 2nd CEAS Specialist Conference on Guidance, Navigation & Control, Delft, The Netherlands, April 10-12, 2013, pp.1110-1121.

[10] M.G.A. Ruizenaar (201*2*). Europian patent ep2492637a1. http://www.epo.org/index.html.

[11] Yigiter Yuksel, Naser El-Sheimy and Aboelmagd Noureldin (2010). Error Modeling and Characterization of Environmental Effects for Low Cost Inertial MEMS Units, in proceedings of the Position Location and Navigation Symposium (PLANS), 2010 IEEE/ION, Indian Wells, California, USA.